

## Core-Corona Separation in Ultrarelativistic Heavy Ion Collisions

Klaus Werner\*

*SUBATECH, University of Nantes-IN2P3/CNRS-EMN, Nantes 44000, France*

(Received 9 March 2006; revised manuscript received 7 February 2007; published 10 April 2007)

Simple geometrical considerations show that the collision zone in high energy nuclear collisions may be divided into a central part (“core”), with high energy densities, and a peripheral part (“corona”), with smaller energy densities, more like in  $pp$  or  $pA$  collisions. We present calculations that allow us to separate these two contributions, and which show that the corona contribution is quite small (but not negligible) for central collisions, but gets increasingly important with decreasing centrality. We will discuss consequences concerning results obtained in heavy ion collisions at the BNL Relativistic Heavy Ion Collider and CERN Super Proton Synchrotron.

DOI: [10.1103/PhysRevLett.98.152301](https://doi.org/10.1103/PhysRevLett.98.152301)

PACS numbers: 25.75.Dw

Nuclear collisions at the Relativistic Heavy Ion Collider (RHIC) are believed to provide sufficiently high energy densities to create a thermalized quark-gluon fireball which expands by developing a strong collective radial flow [1–4]. However, not all produced hadrons participate in this collective expansion: the peripheral nucleons of either nucleus essentially perform independent  $pp$  or  $pA$ -like interactions, with a very different particle production compared to the high density central part. For certain observables, this “background” contribution spoils the “signal”, and to get a detailed understanding of RHIC and Super Proton Synchrotron (SPS) data, we need to separate low and high density parts.

In order to get quantitative results, we need a simulation tool, and here we take EPOS [5], which has proven to work very well for  $pp$  and  $dAu$  collisions at RHIC. EPOS is a parton model, so in case of a AuAu collision there are many binary interactions, each one represented by a parton ladder. Such a ladder may be considered as a longitudinal color field, conveniently treated as a relativistic string. The strings decay via the production of quark-antiquark pairs, creating in this way string fragments—which are usually identified with hadrons. Here, we modify the procedure: we have a look at the situation at an early proper time  $\tau_0$ , long before the hadrons are formed: we distinguish between string segments in dense areas (more than  $\rho_0$  segments per unit area in given transverse slices), from those in low density areas. We refer to high density areas as core, and to low density areas as corona. In Fig. 1, we show an example (randomly chosen) of a semiperipheral (40%–50%) AuAu collisions at 200 GeV (cms), simulated with EPOS.

There is always a contribution from the low density area, but much more importantly, as discussed later, the importance of this contribution depends strongly on particle type and transverse momentum. For central collisions, the low density contribution is obviously less important, for more peripheral collisions this contribution will even dominate.

We adopt the following strategy: the low density part will be treated using the usual EPOS particle production

which has proven to be very successful in  $pp$  and  $dAu$  scattering (the peripheral interactions are essentially  $pp$  or  $pA$  scatterings). For the high density part, we simply try to parameterize particle production, in the most simple way possible (it is not at all our aim to provide a microscopic description of this part).

In practice, we consider transverse slices characterized by some range in  $\eta = 0.5 \ln(t+z)/(t-z)$ . String segments in such a slice move with rapidities very close to  $\eta$ . We subdivide a given slice into elementary cells, count the number of string segments per cell, and determine such for each cell whether it belongs to the core or the corona (bigger or smaller than the critical density  $\rho_0$ ). Connected cells (closest neighbors) in a given slice are considered to be clusters, whose energy and flavor content are completely determined by the corresponding string segments. Clusters are then considered to be collectively expanding: Bjorken-like in longitudinal direction with in addition

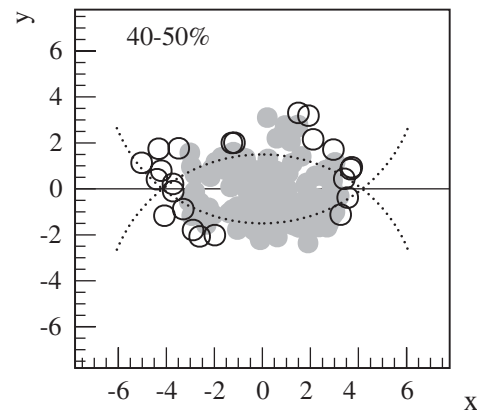


FIG. 1. A Monte Carlo realization of a semiperipheral (40%–50%) AuAu collision at 200 GeV (cms). We show string segments in the core (closed gray circles) and the corona (open circles). The big circles are put in just to guide the eye: they represent the two nuclei in hard sphere approximation. We consider a projection of segments within  $z = \pm 0.4$  fm to the transverse plane  $(x, y)$ .

some transverse expansion. We assume particles to freeze-out (FO) at some given energy density  $\varepsilon_{\text{FO}}$ , having acquired at that moment a collective radial flow. The latter one is characterized by a linear radial rapidity profile from inside to outside with maximal radial rapidity  $y_{\text{rad}}$ . In addition, we impose an azimuthal asymmetry, being proportional to the initial spatial eccentricity  $\epsilon = \langle y^2 - x^2 \rangle / \langle y^2 + x^2 \rangle$ , with a proportionality factor  $f_{\text{ecc}}$ . By imposing radial flow, we have to rescale the cluster mass  $M$  as

$$M \rightarrow M \times 0.5y_{\text{rad}}^2 / (y_{\text{rad}} \sinh y_{\text{rad}} - \cosh y_{\text{rad}} + 1),$$

in order to conserve energy. Hadronization then occurs according to covariant phase space, which means that the probability  $dP$  of a given final state of  $n$  hadrons is given as

$$\prod_{\text{species } \alpha} \frac{1}{n_\alpha!} \prod_{i=1}^n \frac{d^3 p_i g_i s_i}{(2\pi\hbar)^3 2E_i} \frac{M}{\varepsilon_{\text{FO}}} \delta(M - \sum E_i) \delta(\sum \vec{p}_i) \delta_{f, \Sigma f_i},$$

with  $p_i = (E_i, \vec{p}_i)$  being the four-momentum of the  $i$ th hadron,  $g_i$  its degeneracy, and  $f_i$  its quark flavor content ( $u - \bar{u}, d - \bar{d} \dots$ ). The number  $n_\alpha$  counts the number of hadrons of species  $\alpha$ . The term  $M/\varepsilon_{\text{FO}}$  is the cluster proper volume. We use a factor  $s_i = \gamma_s^{\pm 1}$  for each strange particle (sign plus for a baryon, sign minus for a meson), with  $\gamma_s$  being a parameter. We believe that  $s_i$  mimics final state rescattering, but for the moment we can only say that this factor being different from unity improves the fit of the data considerably. The whole procedure perfectly conserves energy, momentum, and flavors (microcanonical procedure).

So the core definition and its hadronization are parameterized in terms of few global parameters (in brackets the values): the core formation time  $\tau_0$  (1 fm), the core formation density  $\rho_0$  (2/fm<sup>3</sup>), the freeze-out energy density  $\varepsilon_{\text{FO}}$  (0.22 GeV/fm<sup>3</sup>), the maximum radial flow  $y_{\text{rad}}$  ( $0.75 + 0.20 \log(\sqrt{s}/200 \text{ GeV})$ ), the eccentricity coefficient  $f_{\text{ecc}}$  (0.45), and the factor  $\gamma_s$  (1.3). At RHIC energies, the final results are insensitive to variations of  $\tau_0$ : even changes as big as a factor of 2 do not affect the results. This is a nice feature, indicating that the very details of the initial state do not matter so much. We call these parameters “global”, since they account for all observables at all possible different centralities and all energies. In the following, we are going to discuss results, all obtained with the above set of parameters.

Our hadronization of the core part is certainly motivated by the remarkable success of statistical hadronization models [6] and blast-wave fits [7,8]. We use covariant statistical hadronization, whereas usually the noncovariant procedure is employed, but the difference is minor. We also impose a collective flow, with an assumed flow profile, as in the blast-wave fit. So the general ideas are the same. However, a really new aspect is the possibility of making a global fit, considering all energies, centralities, and colliding systems with one set of parameters. In the above-

mentioned models one has a set of fit parameters for each of these possibilities. An important new aspect is also the separation of a (collectively behaving) core and a corona contribution, which seems to be very important for understanding the centrality dependence of hadron yields. Finally, our statistical hadronization is based on initial energy densities provided by a parton model (EPOS), which works well for  $pp$  and  $d\text{Au}$  scattering. This fixes the overall multiplicity already within 10%, flow and freeze-out conditions have only a minor effect on this quantity.

All the discussion of heavy ion data will be based on the interplay between core and corona contributions. To get some feeling, we first compare in Fig. 2 the  $m_t$  spectra of pions and lambdas from the core in central (0%–5%) AuAu collisions with the corresponding spectra in  $pp$  scattering (which is qualitatively very similar to the corona contribution). The core spectra are divided by the number of binary collisions. We observe several remarkable features: the shapes of the pion and lambda curves in  $pp$  are not so different, whereas there is much more species dependence in the core spectra, since the heavier particles acquire large transverse momenta due to the flow effect. One observes furthermore that the yields for the two spectra in  $pp$  are much wider spread than the ones from the core; in particular, pion production is suppressed in the core hadronization compared to  $pp$ , whereas lambda production is favored. All this is quite trivial, but several “mysteries” discussed in the literature (and to be discussed later in this Letter) are just due to this.

In Fig. 3, we plot the relative contribution of the core (relative to the complete spectrum, core + corona) as a function of  $m_t - m$ , for different particle species. For central collisions, the core contribution dominates largely, whereas for semicentral collisions (40%–50%) and even more for peripheral collisions the core contribution decreases, giving more and more space for the corona part.

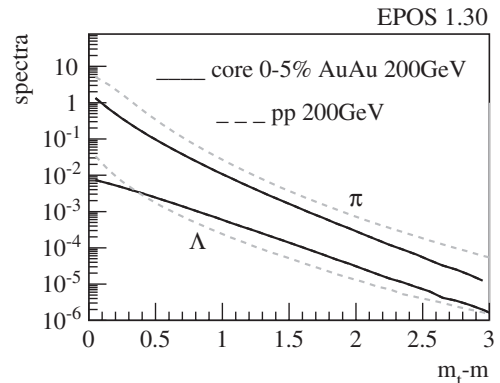


FIG. 2. Invariant yields  $1/2\pi m_t dn/dy dm_t$  of pions and lambdas, for the core contribution corresponding to a central (0%–5%) AuAu collision (full lines) and proton-proton scattering (dashed lines). The core spectra are divided by the number of binary collisions.

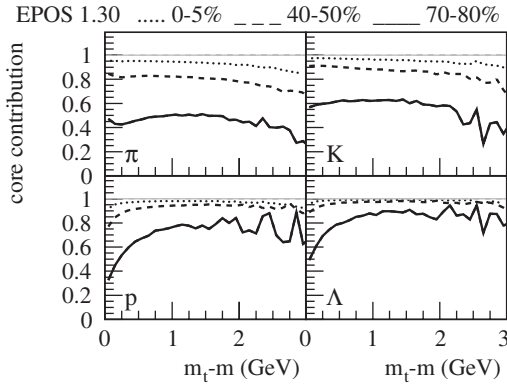


FIG. 3. The relative contribution of the core [core/(core + corona)] as a function of the transverse mass for different hadrons ( $\pi$ ,  $K$ ,  $p$ ,  $\Lambda$ ) at different centralities.

Apart of these general statements, the precise  $m_t$  dependence of the relative weight of core versus corona depends on the particle type.

We are now ready to investigate the data. In Fig. 4, we plot the centrality dependence of the particle yield per participant (per unit of rapidity) in Au + Au collisions at 200 GeV (RHIC), for  $\pi^+$ ,  $K^+$ ,  $p$ ,  $\bar{\Lambda}$ ,  $\Xi^+$ : we show data [9,10] together with the full calculation (quite close to the data), but also indicating the core contribution. In Fig. 5, we show the corresponding results for Pb + Pb collisions at 17.3 GeV (SPS). Concerning the SPS results, we consider  $dn/dy/N_p$  in case of  $K_S$ ,  $\bar{\Lambda}$ , and  $\Xi^+$ , whereas we have  $4\pi$  multiplicities per participant in case of  $\pi^-$  and  $K^-$  (for simulations and data). Whereas central collisions are always clearly core dominated, the core contributes less and less with decreasing centrality. The difference between solid and dotted curves (in other words: the importance of the corona contribution) is bigger at the SPS compared to RHIC, and it is bigger for light particles compared to heavy

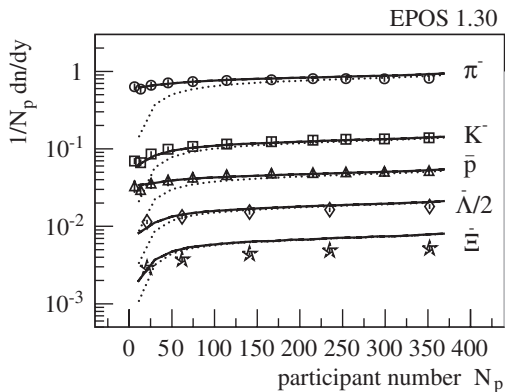


FIG. 4. Rapidity density  $dn/dy$  per participant as a function of the number of participants ( $N_p$ ) in Au + Au collisions at 200 GeV (RHIC) for  $\pi^-$ ,  $K^-$ ,  $\bar{p}$ ,  $\bar{\Lambda}$ ,  $\Xi^+$ . We show data (points) [9,10] together with the full calculation (full lines) and just the core part (dotted lines).

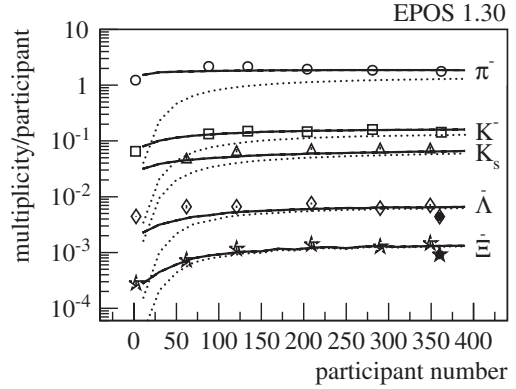


FIG. 5. Multiplicity per participant as a function of the number of participants ( $N_p$ ) in Pb + Pb collisions at 17.3 GeV (SPS) for  $\pi^-$ ,  $K^-$ ,  $K_S$ ,  $\bar{\Lambda}$ ,  $\Xi^+$ . We show data (points) [11-14] together with the full calculation (full lines) and just the core part (dotted lines).

ones. For example, there is a big corona contribution for pions and a very small one for  $\Xi^+$  particles. Also the strength of the centrality dependence depends on the hadron type: for example  $\Xi^+$  particles show a stronger centrality dependence than pions. It seems that the centrality dependence is essentially determined by the relative importance of the corona contribution: the less the corona contributes, the more the yield varies with centrality.

To further investigate the connection between relative corona weight and centrality dependence, we plot in Fig. 6 the centrality dependence of multiplicities per participant for different hadrons, at 200 GeV (RHIC) and 17.3 GeV (SPS), for the core contribution. We observe two universal curves, one per energy. So for a given energy, the core contributions for all the different hadrons show the same centrality dependence. This proves that the different centrality dependencies for the different hadron species are simply due to different core-corona weights. For example,

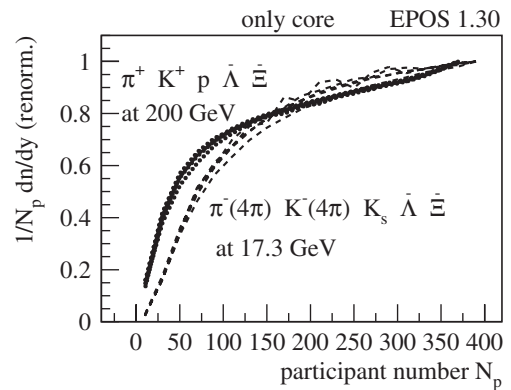


FIG. 6. Multiplicity per participant as a function of  $N_p$  for only the core part. We show results for  $\pi^-$ ,  $K^-$ ,  $\bar{p}$ ,  $\bar{\Lambda}$ ,  $\Xi^+$  in Au + Au collisions at 200 GeV (dotted lines), and for  $\pi^-$ ,  $K^-$ ,  $K_S$ ,  $\bar{\Lambda}$ ,  $\Xi^+$  in Pb + Pb collisions at 17.3 GeV (dashed lines).

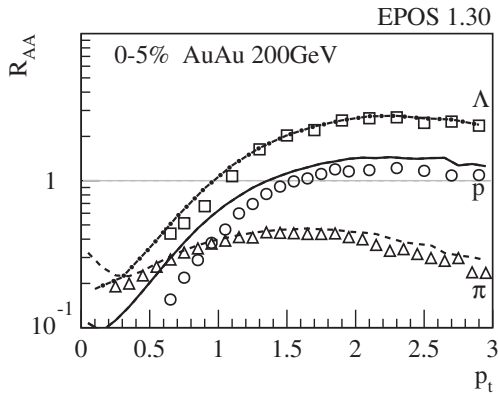


FIG. 7. Nuclear modification factors in central AuAu collisions at 200 GeV. Lines are full calculations, symbols represent data [9,10]. We show results for pions (dashed line; triangles), protons (full line; circles), and lambdas (dashed-dotted line; squares).

the fact that  $\Xi$  particles show a stronger centrality dependence than pions is simply due to the fact that the former ones have less corona admixture than the latter ones.

Lets us come to  $p_t$  spectra. We checked all available  $p_t$  data ( $\pi^+$ ,  $K^+$ ,  $p$ ,  $\bar{\Lambda}$ ,  $\Xi^+$ , for  $p_t \leq 5$  GeV), and our combined approach (core + corona) describes all the data within 20%. Lacking space, we just discuss a (typical) example: the nuclear modification factor ( $AA/pp$ /number of collisions), for  $\pi^+$ ,  $p$ ,  $\bar{\Lambda}$  in central AuAu collisions at 200 GeV; see Fig. 7. For understanding these curves, we simply have a look at Fig. 2, where we compare the core contributions from AuAu (divided by the number of binary collisions) with  $pp$ . Since for very central collisions the core dominates largely, the ratio of core to  $pp$  (the solid lines divided by the dotted ones in Fig. 2) corresponds to the nuclear modification factor. We discussed already earlier the very different behavior of the core spectra (flow plus phase space decay) compared to the  $pp$  spectra (string decay): pions are suppressed, whereas heavier particles like lambdas are favored. Or, better to say it the other way round: the production of baryons compared to mesons is much more suppressed in string decays than in statistical hadronization. This is why the nuclear modification factor for lambdas is different from the one for pions. So what we observe here is nothing but the very different behavior of statistical hadronization (plus flow) on one hand, and string fragmentation on the other hand. This completely statistical behavior indicates that the low  $p_t$  partons get completely absorbed in the core matter.

The  $R_{cp}$  modification factors (central over peripheral) are much less extreme than  $R_{AA}$ , since peripheral AuAu collisions are a mixture of core and corona (the latter one

being  $pp$ -like), so a big part of the effect seen in  $R_{AA}$  is simply washed out.

To summarize, we have discussed the importance of separating core and corona contributions in ultrarelativistic heavy ion collisions. The core-corona separation is realized based on the determination of string densities at an early time. Particle production from the corona is done as in proton-proton scattering, whereas the core hadronization is parameterized in a very simple way, imposing radial flow. The corona contribution is quite small (but not negligible) for central collisions, but gets increasingly important with decreasing centrality. The core shows a very simple centrality dependence: it is the same for all hadron species, at a given bombarding energy. The fact that the centrality dependence of the total hadron yield is strongly species dependent is simply due to the fact that the relative corona contribution depends on the hadron type.

\*Electronic address: werner@subatech.in2p3.fr

- [1] I. Arsene *et al.* (BRAHMS Collaboration), Nucl. Phys. **A757**, 1 (2005).
- [2] K. Adcox *et al.* (PHENIX Collaboration), Nucl. Phys. **A757**, 184 (2005).
- [3] B. B. Back (PHOBOS Collaboration), Nucl. Phys. **A757**, 28 (2005).
- [4] J. Adams *et al.* (STAR Collaboration), Nucl. Phys. **A757**, 102 (2005).
- [5] K. Werner, F. M. Liu, and T. Pierog, Phys. Rev. C **74**, 044902 (2006).
- [6] P. Braun-Munzinger, I. Heppe, and J. Stachel, Phys. Lett. B **465**, 15 (1999); F. Becattini, J. Manninen, and M. Gazdzicki, Phys. Rev. C **73**, 044905 (2006); J. Cleymans, H. Oeschler, K. Redlich, and S. Wheaton, Phys. Rev. C **73**, 034905 (2006); J. Rafelski and M. Danos, Phys. Lett. B **97**, 279 (1980); J. Rafelski and J. Letessier, J. Phys. G **28**, 1819 (2002).
- [7] E. Schnedermann, J. Sollfrank, and U. Heinz, Phys. Rev. C **48**, 2462 (1993).
- [8] F. Retiere, J. Phys. G **30**, S827 (2004); J. Adams (STAR Collaboration) Phys. Rev. Lett. **92**, 112301 (2004); I. Kraus (NA49 Collaboration), J. Phys. G **31**, S147 (2005).
- [9] S. S. Adler *et al.* (PHENIX Collaboration), Phys. Rev. C **69**, 034909 (2004).
- [10] J. Adams *et al.* (STAR Collaboration), Phys. Rev. Lett. **98**, 062301 (2007).
- [11] J. Bachler *et al.* (NA49 Collaboration), Nucl. Phys. **A661**, 45 (1999).
- [12] F. Antinori *et al.* (NA57 Collaboration), J. Phys. G **32**, 427 (2006).
- [13] S. V. Afanasiev *et al.* (NA49 Collaboration), Phys. Lett. B **538**, 275 (2002).
- [14] T. Anticic *et al.* (NA49 Collaboration), Phys. Rev. Lett. **93**, 022302 (2004).